High Efficiency Narrow-Bore Columns Packed with 1.6 and 2.7 µm Solid Core Particles

By Thomas H. Walter, Stephen Shiner, Gary Izzo, Michael Savaria, Pamela C. Iraneta, Ken Berthelette, Jonathan P. Danaceau, Erin E. Chambers and Kenneth J. Fountain
Waters Corporation, 34 Maple Street, Milford, MA 01757, USA

It has previously been shown that it is possible to obtain remarkably high efficiencies for standard-bore (4.6 mm diameter) columns packed with 2.6 – 2.7 µm solid-core particles (SCP). Minimum reduced plate heights of 1.3 – 1.6 have been reported for these columns. However, similarly low reduced plate heights have been much more difficult to achieve for 2.6 – 2.7 µm SCP in narrow-bore (2.1 mm diameter) columns. Packing < 2 µm SCP into narrow-bore columns has proven to be even more challenging. In this article, we demonstrate that it is possible to achieve reduced plate heights of 1.5 – 1.6 for 2.7 and 1.6 µm SCP in narrow-bore columns. Examples are shown to demonstrate that these high efficiencies may provide faster or higher resolution separations.

One of the most discussed recent advances in columns for HPLC and UPLC is the use of solid-core particles (SCP) instead of fully porous particles (FPP) [1 - 9]. Remarkably high optimum efficiencies have been reported for standard-bore (4.6 mm diameter) columns packed with 2.6 or 2.7 µm SCP, in the range of 230,000 – 300,000 plates per meter [2, 5]. Expressed as reduced plate heights (h), a measure of efficiency that is normalised for differences in particle size, these efficiencies translate to h values in the range of 1.3 – 1.6. The reduced plate height is inversely proportional to efficiency, so low h values correspond to high efficiencies for a given particle size. For comparison, standard-bore columns packed with similar size FPP typically have reduced plate heights in the range of 1.8 – 2.2 [1]. The lower h values of columns packed with SCP have been shown to arise primarily from reductions in longitudinal diffusion and eddy dispersion [2].

Achieving similarly high efficiencies for narrow-bore (2.1 mm diameter) columns has proven to be more difficult. Narrow-bore columns are preferred for use with mass spectrometry (MS) detection because their lower optimum flow rates are a better match for electrospray ionisation [10]. Narrow-bore columns are also attractive for use with optical detectors because they give higher sensitivity when the same mass of analyte is injected as on a standard-bore column [11]. Narrow-bore columns also use much less mobile phase. The consumption of mobile phase is reduced by a factor of 4.8 for 2.1 mm vs 4.6 mm diameter columns operated at the same linear velocity.

Several investigations of the performance of 2.6 or 2.7 µm SCP in narrow-bore columns have reported optimum efficiencies in the range of 160,000 – 250,000 plates per meter, corresponding to reduced plate heights of 1.5 – 2.5 [2, 4, 5, 12]. This places them in the range of narrow-bore columns packed with 2.5 µm FPP [13]. It has been shown that narrow-bore columns packed with 2.6 or 2.7 µm SCP have greater eddy dispersion than their standard-bore counterparts, which is the major cause of their lower efficiencies [12]. More specifically, the increased trans-column contribution to the eddy dispersion is the issue for the narrow-bore columns. The trans-column eddy dispersion is a measure of the radial homogeneity of the packed bed structure. The radial homogeneity is affected by the column packing process, and may be improved by optimisation of the packing conditions.

The difficulty of column packing optimisation increases not only with decreasing column diameter, but also with decreasing particle size. Minimum reduced plate heights of 1.9 - 2.9 have been reported for 1.7 µm SCP in narrow-bore columns [3, 5, 12, 14]. We have worked to optimise the packing of narrow bore columns with < 2 µm particles over the last ten years, since the introduction of UPLC® [15]. With the knowledge gained from packing < 2 µm FPP, we have been able to achieve reduced plate heights for SCP narrow bore columns that are similar to the remarkable values previously reported for 2.6 or 2.7 µm SCP standard-bore columns. In this article, we report examples of the efficiencies and reduced plate heights that we have achieved for narrow bore columns packed with 1.6 and 2.7 µm SCP. Examples are also shown to demonstrate the benefits of these higher efficiencies for increasing separation speed and resolution.

Experimental

SCP columns were packed with 1.6 or 2.7 µm CORTECS® silica particles (Waters Corp, Milford, MA, USA). Relevant characteristics of these particles are summarised in Table 1. The particle size distributions of these particles were determined using a Coulter Multisizer 3 (Beckman Coulter, Brea, CA, USA). The average particle sizes from

Material	Morphology	Average Particle Size (µm)	Pore Volume (cm^3/g)	Surface Area (m^2/g)	Average Pore Diameter (Å)
2.7 µm CORTECS C_{18}	Solid-core ρ = 0.70	2.64	0.26	100	90
1.6 µm CORTECS C_{18}	Solid-core ρ = 0.70	1.61	0.26	100	90
1.7 µm SCP C_{18}	Solid-core ρ = 0.73	1.80	0.24	98	86
1.7 µm FPP C_{18}	Fully porous	1.87	0.70	185	130

Table 1: Characteristics of the Particles (ρ is the ratio of the core diameter to the particle diameter)

the volume-weighted distributions were used to calculate reduced plate heights. The pore volumes, surface areas and average pore diameters of the unbonded particles were determined using an ASAP 2420 Multipoint N2 Sorption Analyzer (Micromeritics, Norcross, GA, USA). The columns were tested using ACQUITY UPLC® I-Class systems (Waters Corp, Milford, MA, USA). To achieve flow rates over 2 mL/min for the 4.6 mm diameter columns, an ACQUITY system was used with two solvent managers connected in parallel. Efficiencies were calculated at different flow rates for acenaphthene, using a 75/25 (v/v) acetonitrile/water mobile phase and a temperature of 30°C. Thiourea was used as the unretained (t_0) marker, and t_0 values were corrected for the system delay time. The retention factors for acenaphthene ranged between 2 and 3 for the columns tested. A tunable UV detector equipped with a 500 nL flow cell was used, set to a wavelength of 254 nm and a sampling rate of 80 Hz. A fixed loop injector was used, fitted with a 1.0 µL sample loop. We report the USP efficiencies, with no correction made for extra-column dispersion. Reduced plate heights (h) were calculated as: $h = L/(N\ d_p)$

where L is the column length, N is the measured efficiency and d_p is the average particle diameter. Linear velocities (u_0) were calculated as: $u_0 = L/t_0$

Reduced linear velocities (**v**) were calculated as: $\mathbf{v} = u_0 d_p / D_M$

where D_M is the diffusion coefficient of the analyte in the mobile phase. The D_M value of acenaphthene was calculated using the average of the Wilke-Chang and Scheibel equations [16]. Specific column permeabilities (K_V) were calculated as: $K_V = u_0 \eta L/\Delta P$

where η is the viscosity of the mobile phase and ΔP is the pressure drop across the column (the total pressure less the system pressure). Peak capacities (P_c) were calculated as: $P_c = 1 + (t_g/w)$

where t_g is the gradient time and w is the average peak width measured at 13.4% of the peak height (equal to 4σ where σ is the standard deviation or variance of the peak).

The sulpha drugs were purchased from Sigma-Aldrich (St. Louis, MO, USA). The synthetic cannabinoids were obtained from Cerilliant (Round Rock, TX, USA) and Cayman Chemical (Ann Arbor, MI, USA). The synthetic cannabinoids were detected using a Xevo TQD Mass Spectrometer (Waters, Milford, MA, USA) with electrospray positive ionisation. Multiple reaction monitoring was used, with the collision energy and cone voltage optimised for each compound (see Table 2). The capillary voltage was 1 kV.

Compound	Formula	MRM Transition	Cone Voltage (V)	Collision Energy (eV)
AM-2233	$C_{22}H_{23}IN_2O$	459.2 → 98.0	48	50
RCS-4,M10	$C_{20}H_{21}NO_3$	324.2 → 121.0	40	36
RCS-4,M11	$C_{20}H_{19}NO_3$	322.2 → 121.0	42	32
AM-1248	$C_{26}H_{34}N_2O$	391.4 → 135.1	62	42
JWH-073 4-butanoic acid metabolite	$C_{23}H_{19}NO_3$	358.2 → 155.1	52	32
JWH-073 4-hydroxybutyl metabolite	$C_{23}H_{21}NO_2$	344.2 → 155.1	52	32
JWH-018 5-pentanoic acid metabolite	$C_{24}H_{21}NO_3$	372.2 → 155.1	54	32
JWH-073 (+/-) 3-hydroxybutyl metabolite	$C_{23}H_{21}NO_2$	344.2 → 155.1	54	36
JWH-018 5-hydroxypentyl metabolite	$C_{24}H_{23}NO_2$	358.2 → 155.1	50	24
JWH-018 (+/-) 4-hydroxypentyl metabolite	$C_{24}H_{23}NO_2$	358.2 → 155.1	50	34

Table 2: Molecular Formulae and MS Conditions for Synthetic Cannabinoids

Results and Discussion

Efficiencies were determined as a function of flow rate for 2.7 µm CORTECS C18 in 50 mm long columns with diameters of 2.1, 3.0 and 4.6 mm. The results are shown in Figure 1 as plots of efficiency vs linear velocity. All three columns show similar results, with maximum efficiencies ranging from 12,800 – 13,100 (256,000 – 262,000 plates per meter). The same results are shown in Figure 2 as plots of reduced plate height vs reduced linear velocity. The minimum reduced plate heights range from 1.41 – 1.45. These are in the range previously reported only for standard-bore columns. These results demonstrate that with optimised column packing, similar efficiencies may be obtained for 2.7 µm SCP in standard-bore and narrow-bore columns. It is important to note that extra-column dispersion may have a significant impact on measured column efficiencies, particularly for narrow-bore columns [7 - 9]. The UPLC system used for these measurements has the lowest extra-column dispersion variance currently available (1.0 µL^2) [7]. The calculated effect of extra-column dispersion on the optimum efficiency of these columns is -3.5% for the 2.1 mm column, -0.9% for the 3.0 mm column and -0.2% for the 4.6 mm column.

Efficiencies were determined as a function of flow rate for 1.6 µm CORTECS C18 in a 2.1 x 50 mm column. For comparison, a 1.7 µm FPP column and a 1.7 µm SCP column were

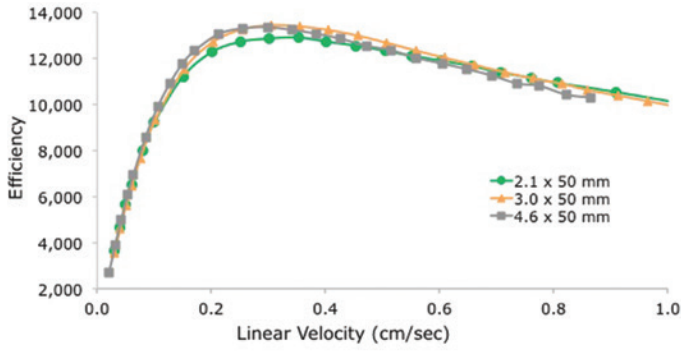

Figure 1: Plots of efficiency vs linear velocity for 50 mm long columns of different diameters packed with 2.7 µm CORTECS C18 (circles: 2.1 mm, triangles: 3.0 mm, squares: 4.6 mm). The analyte was acenaphthene, the mobile phase was 75/25 v/v acetonitrile/ water and the temperature was 30°C.

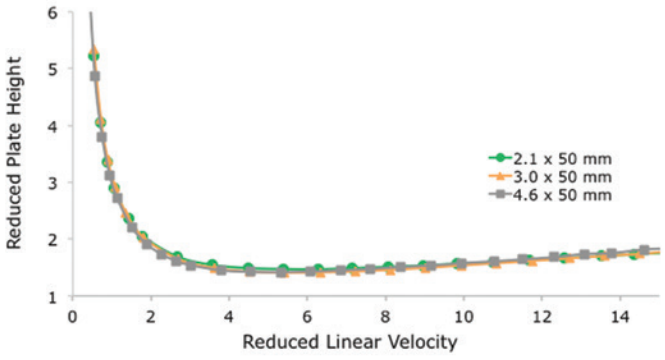

Figure 2: Plots of reduced plate height vs reduced linear velocity for the three columns of Figure 1.

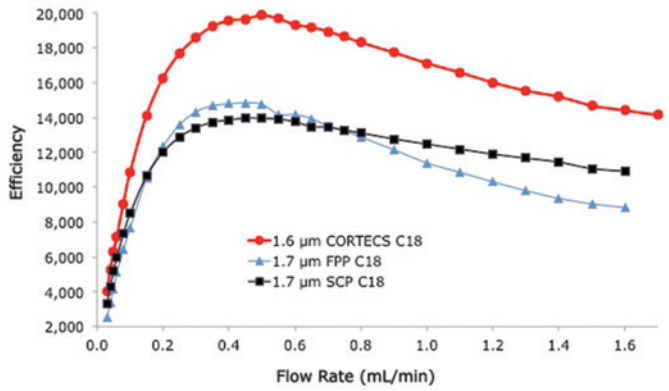

Figure 3: Plots of efficiency vs flow rate for 2.1 x 50 mm columns packed with different materials (circles: 1.6 µm CORTECS C18, triangles: 1.7 µm FPP C18, squares: 1.7 µm SCP C18). The analyte was acenaphthene, the mobile phase was 75/25 v/v acetonitrile/ water and the temperature was 30°C.

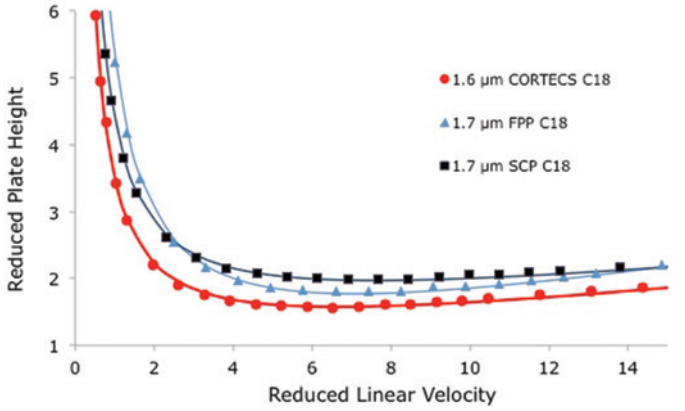

Figure 4: Plots of reduced plate height vs reduced linear velocity for the three columns of Figure 3.

also tested. Shown in Figure 3 are plots of efficiency vs flow rate for the three columns. The results show that the 1.6 µm CORTECS C18 column has the highest efficiencies at all flow rates. The optimum efficiency is 32% higher than that of the 1.7 µm FPP column and 40% higher than that of the 1.7 µm SCP column. The optimum efficiency for the 1.6 µm CORTECS C18 column approaches 400,000 plates per meter. These results are shown as plots of reduced plate height vs reduced linear velocity in Figure 4. The 1.6 µm CORTECS C18 column shows the lowest reduced plate heights, with a minimum value of 1.52. This value is only 5% higher than that of the narrow-bore 2.7 µm CORTECS C18 column. The calculated effect of extra-column dispersion on the optimum efficiency of this column is -5.2%.

Several factors contribute to the higher efficiency of the 1.6 µm CORTECS column. The smaller size of the 1.6 µm CORTECS particles relative to the particles in the other columns account for increases of 12 – 16%. The nominal 1.7 µm particles were found to have average particle diameters of 1.80 (SCP) and 1.87 µm (FPP). Most of the efficiency increase vs the FPP column comes from the solid-core particle morphology. This is evident by comparing the terms of the reduced van Deemter equation obtained by fitting the data of Figure 4 to the following equation:

$h = A + B/v + Cv$

The coefficients for the three columns are given in Table 3. The CORTECS column shows lower B and C values than the FPP column. The lower B coefficient (longitudinal diffusion) is a result of the lower pore volume of the CORTECS particles [2]. The lower C value is believed to be due to decreased band broadening from radial temperature gradients resulting from the higher thermal conductivity of the packed bed of solid-core particles [2, 14]. Comparing the 1.6 µm CORTECS column to the 1.7 µm SCP column, the CORTECS column has a lower A term (eddy dispersion) and a slightly lower B term. The lower A term results from the more homogeneous packed bed structure in the CORTECS column.

In addition to efficiency, permeability is an important column parameter. Column pressure is inversely related to permeability. In Figure 5, plots of column pressure vs. flow rate for the four 2.1 x 50 mm columns that we evaluated for efficiency are shown. The specific permeabilities of these columns are shown in Table 4. As expected, the 2.7 µm CORTECS C18 column has a permeability that is 2.6 times that of the 1.6 µm CORTECS C18 column, since permeability is proportional to the square of the particle size [17]. It is notable that the 1.6 µm CORTECS C18 column has a higher permeability than the 1.7 µm FPP column. There are two reasons for this surprising result. Firstly, the CORTECS particles have a narrower particle size distribution than the fully porous particles. Secondly, the CORTECS column has a higher interstitial porosity than the FPP column. This has been observed for other SCP columns, and has been attributed to the rough surface morphology of most solid-core particles [2].

In addition to the higher optimum efficiency of the 1.6 µm CORTECS C18 column, it is evident in Figure 3 that the efficiency of this column declines more slowly above the optimum flow rate, relative to the FPP column. This is reflected in the lower C term in the reduced van Deemter curve for the 1.6 µm CORTECS C18 column. This may be exploited to obtain faster separations, by operating at a higher flow rate than used for FPP columns of the same diameter. An example is shown in Figure 6 for the separation of seven sulpha drugs. These analytes were separated using an acetonitrile gradient on 2.1 x 50 mm columns packed with two different materials. The top chromatogram was obtained using a 1.7 µm FPP C18 column, a 5.0 min gradient and a flow rate of 0.5 mL/min. The middle chromatogram was obtained using a 1.6 µm CORTECS C18 column under the same conditions. The bottom chromatogram was obtained using a 1.6 µm CORTECS C18 column, a 2.5 min gradient and a flow rate of 1.0 mL/min. The peak capacities for the three separations were 178 (1.7 µm FPP), 218 (1.6 µm CORTECS C18 with a 5.0 min gradient) and 172 (1.6 µm CORTECS C18 with a 2.5 min gradient). The separation could be carried out on the 1.6 µm CORTECS C18 column in half the time, while still achieving a similar peak capacity as the separation on the 1.7 µm FPP column.

An example that demonstrates the higher efficiency of a 1.6 µm CORTECS C18 column relative to a 1.7 µm FPP C18 column is shown in Figure 7. Ten synthetic cannabinoids were

Column	A	B	C
1.6 µm CORTECS C18	0.77 ± 0.02	2.70 ± 0.02	0.061 ± 0.001
1.7 µm FPP C18	0.38 ± 0.03	4.92 ± 0.03	0.098 ± 0.002
1.7 µm SCP C18	1.12 ± 0.02	3.26 ± 0.02	0.056 ± 0.002

Table 3: Reduced van Deemter Terms for Three 2.1 x 50 mm Columns [Acenaphthene, 75/25 (v/v) acetonitrile/ water, 30°C]

Column	K_V (cm^2)
2.7 µm CORTECS C18	1.34×10^{-10}
1.6 µm CORTECS C18	5.10×10^{-11}
1.7 µm FPP C18	3.95×10^{-11}
1.7 µm SCP C18	5.59×10^{-11}

Table 4: Specific Permeabilities of Four 2.1 x 50 mm Columns

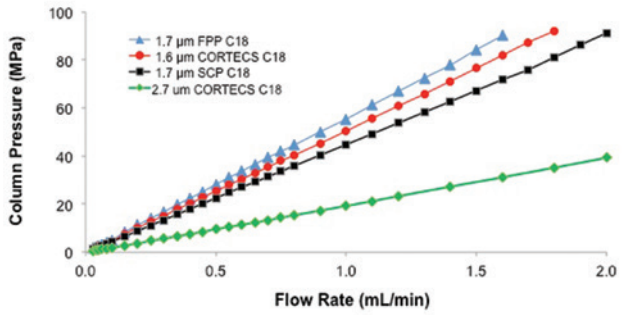

Figure 5: Plots of column pressure vs. flow rate for the three columns of Figure 3 and the 2.7 µm CORTECS C18 2.1 x 50 mm column of Figure 1.

separated using an acetonitrile gradient on 2.1 x 100 mm columns. The peaks were detected using electrospray tandem mass spectrometry. The top chromatogram was obtained using a 1.7 µm FPP C18 column, and shows poor resolution for three peak pairs: 5 and 6, 7 and 8 and 9 and 10. The compounds giving rise to peaks 9 and 10 have the same molecular weight, and cannot be distinguished by mass spectrometry. The bottom chromatogram was obtained using a 1.6 µm CORTECS C18 column. Due to the higher efficiency of this column and slight selectivity differences, the resolution is significantly improved for all three critical pairs. With the higher resolution of peaks 9 and 10, these isobaric compounds may be accurately quantified using a 1.6 µm CORTECS C18 column.

Conclusions

These results demonstrate that it is possible to achieve reduced plate heights of 1.5 – 1.6 for 1.6 and 2.7 µm SCP in narrow-bore columns. Thus, the same improvement in efficiency over FPP columns that was previously demonstrated for 2.6 – 2.7 µm SCP in standard-bore columns is now available in narrow-bore columns. These high efficiency columns may be used to shorten analysis times by increasing the flow rate and/or by using shorter columns. Alternatively, the columns may be operated near their optimum flow rates to achieve higher resolution resulting from their higher maximum efficiencies.

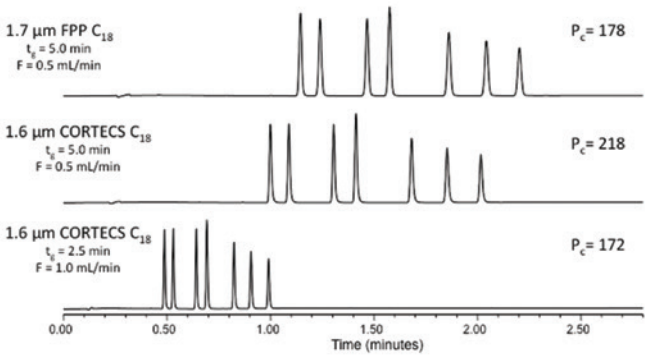

Figure 6: Separations of seven sulpha drugs obtained using two different 2.1 x 50 mm columns (top: 1.7 µm FPP C18, middle and bottom: 1.6 µm CORTECS C18. Mobile phase A was 0.1% formic acid in water, mobile phase B was 0.1% formic acid in acetonitrile and a linear gradient was used from 5 – 60% B. For the top and middle chromatograms the gradient time was 5.0 min and the flow rate was 0.5 mL/min. For the bottom chromatogram the gradient time was 2.5 min and the flow rate was 1.0 mL/min. The sample was an aqueous solution containing 10 µg/mL each of sulfathiazole, sulfamerazine, sulfamethazine, sulfamethoxypyridazine, sulfachloropyridazine, sulfamethoxazole and sulfisoxazole. The injection volume was 4 µL. A PDA detector was used and the column temperature was 30°C.

Acknowledgements

The authors acknowledge Kevin Wyndham, Dan Walsh and Babajide Okandeji for the synthesis of the CORTECS particles, Yuehong Xu for the particle characterisation data and Mia Summers for the planning of the sulpha drug separations.

References

1. J. J. DeStefano, T. J. Langlois, J. J. Kirkland, J. Chromatogr. Sci. 46 (2007) 254.

2. G. Guiochon, F. Gritti, J. Chromatogr. A 1218 (2011) 1915.

3. J. O. Omamogho, J. D. Glennon, Anal. Chem. 83 (2011) 1547.

4. J. Ruta, D. Zurlino, C. Grivel, S. Heinisch, J.-L. Veuthey, D. Guillarme, J. Chromatogr. A 1228 (2012) 221.

5. S. Fekete, E. Oláh, J. Fekete, J. Chromatogr. A 1228 (2012) 57.

6. S. Fekete, D. Guillarme, M. W. Dong, LC-GC N. Am. 32 (2014) 2.

7. T. H. Walter, R. W. Andrews, Trends in Anal. Chem. 63 (2014) 14.

8. F. Gritti, G. Guiochon, . Chromatogr. A 1333 (2014) 60.

9. B. Bobály, D. Guillarme, S. Fekete, J. Sep. Sci. 37 (2014) 189.

10. J. Abian, A. J. Oosterkamp, E. Gelpi, J. Mass Sprectrom. 34 (1999) 244.

11. U. Neue. HPLC Columns – Theory, Technology, and Practice. Wiley-VCH, Inc. New York, 1997, pp. 49 – 53.

12. F. Gritti, G. Guiochon, J. Chromatogr. A 1218 (2011) 1592.

13. D. R. McCabe, P. C. Iraneta, T. H. Walter, Chromatography Today 5 (2012) 32.

14. F. Gritti, G. Guiochon, J. Chromatogr. A 1217 (2010) 5069.

15. J. R. Mazzeo, U. D. Neue, M. Kele, R. Plumb, Anal. Chem. 77 (2005) 460A.

16. J. Li, P. W. Carr, Anal. Chem. 69 (1997) 2530.

17. U. Neue. HPLC Columns – Theory, Technology, and Practice. Wiley-VCH, Inc. New York, 1997, pp. 29 – 33.

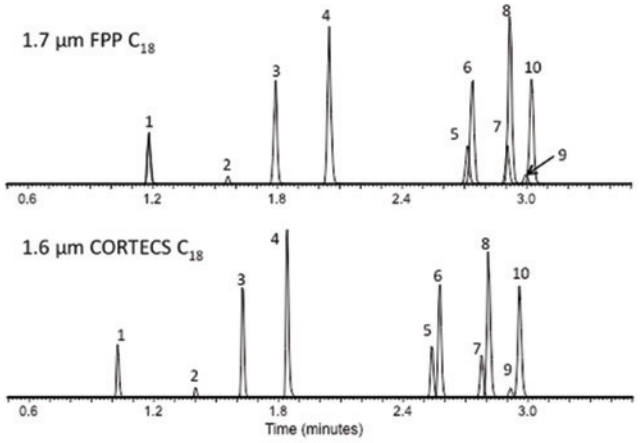

Figure 7: Chromatograms of ten synthetic cannabinoids obtained using two different 2.1 x 100 mm columns (top: 1.7 µm FPP C18, bottom: 1.6 µm CORTECS C18). Mobile phase A was 0.1% formic acid in water and mobile phase B was 0.1% formic acid in acetonitrile. The mobile phase composition initially was 30% B, was increased linearly to 50% B over 2 min, held for 1 min, then increased linearly to 90% B over 4 min. The flow rate was 0.6 mL/min and the column temperature was 30°C. Electrospray MS/MS detection was used. The sample contained AM-2233 (1), RCS-4,M10 (2), RCS-4,M11 (3), AM-1248 (4), JWH-073 4-butanoic acid metabolite (5), JWH-073 4-hydroxybutyl metabolite (6), JWH-018 5-pentanoic acid metabolite (7), JWH-073 3-hydroxybutyl metabolite (8), JWH-018 5-hydroxypentyl metabolite (9) and JWH-018 4-hydroxypentyl metabolite (10).